Determination of anisotropy constants via fitting of magnetic hysteresis to numerical calculation of Stoner–Wohlfarth model

Cite as: AIP Advances 11, 085111 (2021); doi: 10.1063/5.0051454
Submitted: 6 April 2021 • Accepted: 28 July 2021 •
Published Online: 5 August 2021

S. F. Peterson[a] and Y. U. Idzerda[b]

AFFILIATIONS

Department of Physics, Montana State University, Bozeman, Montana 59717, USA

[a]Author to whom correspondence should be addressed: seanpeterson9@montana.edu
[b]Electronic mail: idzerda@montana.edu

ABSTRACT

Anisotropy constants of magnetic materials are typically determined through angle-resolved Ferromagnetic Resonance (ar-FMR) and torque magnetometry, which can be time consuming measurements, thus limiting their utility. The Stoner–Wohlfarth model can be used to numerically fit measured magnetic hysteresis curves to more easily determine these anisotropy constants. To demonstrate this, 10 nm bct $Fe_xCo_yMn_z$ single-crystal films grown by molecular beam epitaxy on MgO(001) substrates were investigated. The hysteresis behavior measured by vibrating sample magnetometry was least-squares fit against numerically calculated hysteresis curves generated from the Stoner–Wohlfarth model to extract the anisotropy constants. The cubic anisotropy of different compositions of FeCoMn films was at ~ 10^4 J/m^3, which is on the same order of magnitude of bct Fe and Co thin films measured by ar-FMR and torque magnetometry techniques.

I. INTRODUCTION

Anisotropic magnetic materials have applications in many forms of magnetic memory, ranging from hard drive technologies to magnetic RAM (MRAM).[1,2] The stability of a bit to thermal fluctuations depends on its total moment, its total magnetic anisotropy, and any fringing magnetic fields from nearby bits. The information density of magnetic memory storage devices can be increased by enhancing the magnetization density of the bit material or by increasing the strength of that material's magnetic anisotropy.[3] Recently, single-crystal bct films of FeCoMn have been synthesized, which greatly increases the magnetization density beyond the Slater-Pauling limit,[4] but the magnetic anisotropy of these ternary films is yet to be fully explored.

Historically, the strength of the magnetic anisotropy was determined by either performing angle-resolved Ferromagnetic Resonance (ar-FMR)[5] or by torque magnetometry.[6] Unfortunately, such measurements are time intensive and not suitable to combinatoric methods where large sample composition ranges can be explored and appropriately mapped as a function of composition. Hysteresis loops measured using the surface magneto-optical Kerr Effect (SMOKE) have been successfully used in a combinatorics study to identify the ferromagnetic region of the ternary phase diagram for sputtered polycrystalline FeCoV films.[7] Similarly, combinatoric synthesis coupled with Vibrating Sample Magnetometry (VSM) has been used to map the coercive field variation over the ternary composition space of FeCoW[8] and FeCoNb[9] films for applications as low-cost alternatives to rare-earth permanent magnets. Although the primary focus of these combinatoric studies was controlling the coercive field values through the alloys' composition, it was found that the coercive field was also dependent on extrinsic surface/interface roughness.[10,11]

Intrinsic anisotropy constants could be a more useful measure of the magnetic utility and can be determined directly from a comparison of the magnetic hysteresis with calculated loops predicted within the Stoner–Wohlfarth (SW) model. This process could be further improved by using the data from existing combinatorics studies to train a machine-learning algorithm[12] to predict alloys with more desirable material parameters, such as higher magnetization densities and anisotropy constants (as was carried out to predict larger magnetic moments through the addition of Pt and Ir to FeCo alloys[13]).

II. MODEL GEOMETRY

The Stoner–Wohlfarth (SW) model is applicable to any sample geometry, but the fitting algorithm can be greatly simplified by selecting particular measurement geometries that exploit the dominant anisotropy within the material (from crystalline or shape anisotropy). By restricting the applied field to be coincident with selected crystallographic directions, specific anisotropy constants can be more easily determined. In the general case (or where there is no dominant anisotropy), vector magnetometry can be used to simultaneously determine all anisotropy constants from numerically fitting multiple hysteresis loops.

The samples in this work are single-crystal 10–20 nm thick bct $Fe_xCo_yMn_z$ thin films deposited on MgO(001) by Molecular Beam Epitaxy (MBE) and capped with 3 nm of Al to prevent oxidation. These films have a large perpendicular anisotropy, confining the magnetization to be within the film plane. Restricting the applied field to the film plane allows for determination of the in-plane cubic anisotropy constants.

The focus of this work is on the first-order cubic anisotropy term, K_1, but the second-order term, K_2 (typically smaller by an order of magnitude), can be likewise determined. By depositing these films on a MgO(001) substrate, the epitaxial nature of the films and the in-plane geometry of the applied field eliminate the contribution of the second-order term. The second-order term does become important for field sweeps taken out of the film plane, especially for field sweeps along the [111] direction.[14] Even in those cases where the magnetization canted out of the film plane, it has been shown[15] that the effect of the K_2 term on the magnetic hysteresis loop is minimal unless K_2 is orders of magnitude larger than K_1.

III. STONER–WOHLFARTH MODEL

Using the geometry seen in Fig. 1, it is possible to construct an energy that incorporates the in-plane cubic anisotropy and the coupling between the applied magnetic field and the magnetization. Using the macroscopic spin approximation, the film magnetization is viewed as a single magnetic domain with a constant magnitude but variable direction. This approximation works well for thin film single-crystal samples that have been previously magnetized to their saturation magnetization. The dominant terms of the energy for such a system are

$$E = K_1 \sin^2\phi\cos^2\phi - \mu_0\vec{H}\cdot\vec{M}, \tag{1}$$

where the first term is the first-order cubic anisotropy energy of constant K_1 and the second is the Zeeman energy. As discussed above, the second-order cubic anisotropy constant, K_2, has been neglected but can be similarly determined if hysteresis measurements are taken in (or near) the [111] plane. This can be rewritten in terms of the reduced energy Γ, by normalizing E by K_1,

$$\Gamma = \sin^2\phi\cos^2\phi - 2\vec{h}\cdot\vec{M}/M_S, \tag{2}$$

where the reduced field $\vec{h} = \frac{\vec{H}}{H_K}$, $H_K = \frac{2K_1}{\mu_0 M}$, $\vec{M}$ is the magnetization vector, and M_S is the saturation magnetization. The most energetically favorable orientation for the magnetization direction, ϕ, is determined from $\frac{\partial\Gamma}{\partial\phi} = 0$ and $\frac{\partial^2\Gamma}{\partial\phi^2} > 0$ at every value of the normalized applied magnetic field (h) and at a particular sweep field direction (θ), which is held constant.

These energy minima for the magnetization direction as a function of the applied magnetic field strength can be seen in Fig. 2 as red shaded curves. The blue shaded curves have negative second-derivatives and are unstable energy maxima. The normalized hysteresis loop is simply the cosine of the angle between the applied magnetic field and the magnetization $[\hat{h}\cdot\vec{M}/M_S = \cos(\phi-\theta)]$ and is shown in Fig. 3.

The minor loops present in the model hysteresis are indicative of a two-step hysteresis, an effect which was measured experimentally by Daboo.[16] These minor loops were theoretically treated by

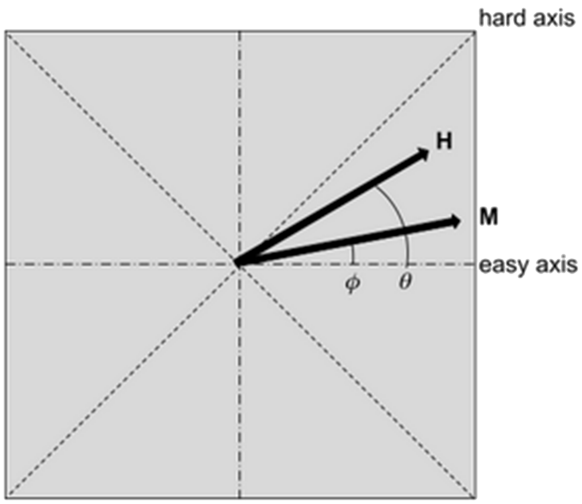

FIG. 1. Thin film magnet with an in-plane cubic anisotropy and $K_1 > 0$. ϕ is the angle between the x-axis and the magnetization direction, and θ is the angle between the x-axis and the applied magnetic field direction.

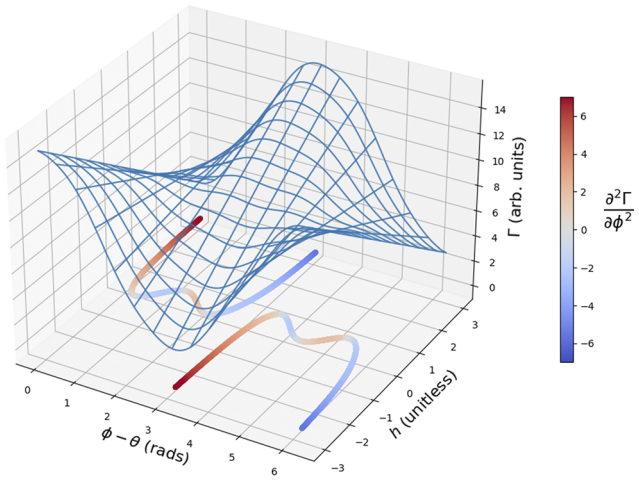

FIG. 2. Normalized energy surface for Eq. (2) at a constant $\theta = \frac{\pi}{12}$, with $\phi(h)$ when $\frac{\partial\Gamma}{\partial\phi} = 0$ is plotted on the bottom plane and shaded proportional to $\frac{\partial^2\Gamma}{\partial\phi^2}$.

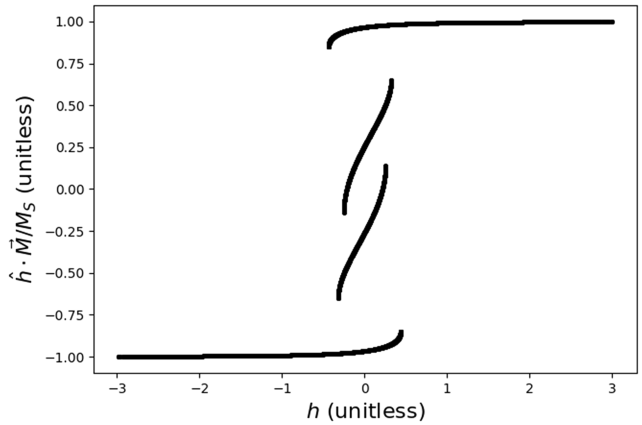

FIG. 3. Magnetic hysteresis of the thin film magnet when $\theta = \frac{\pi}{12}$, with two-step hysteresis, which gets removed when fitting to data.

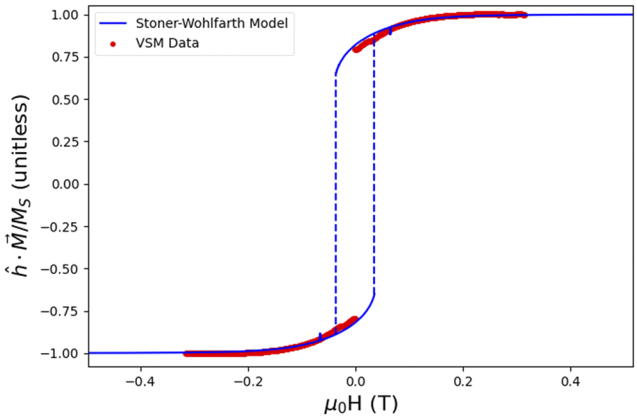

FIG. 4. Stoner–Wohlfarth model best fit to magnetic hysteresis data.

Usov[17] for bulk materials with cubic anisotropies with three equivalent crystalline directions (x, y, and z) whereas the samples considered in this work only have two magnetically equivalent directions due to a tetragonal distortion and the thin film magnetic shape anisotropy, which violate the cubic symmetry in the z-direction.

Historically, the agreement between the Stoner–Wohlfarth model hysteresis loop (using known magnetization and magnetic anisotropy constants) and the measured hysteresis loop was used to validate the SW model.[18] This model can be applied to any sample geometry, as has been carried out for fcc Co nanoparticles[19] and magnetic spin valves,[18] the latter of which include an additional energy term for the magnetic interaction between two magnetic layers of the spin-valve. The process used to validate the SW model can also be inverted to determine the magnetization and magnetic anisotropy constants through a least-squares fitting method. Measured hysteresis loops are the projection of the magnetization vector along the analysis direction. If the analysis direction coincides with the applied field direction (as is typically carried out), the normalized hysteresis loop is again the cosine of the angle between the applied magnetic field and the magnetization.

IV. RESULTS

Residuals between the calculated Stoner–Wohlfarth model magnetizations for a given θ and H_K are found and used in a least-squares fitting algorithm to fit to the model parameters. A typical fit of this type can be seen in Fig. 4. The cubic anisotropy constant can be calculated with the definition of $H_K = \frac{2K_1}{\mu_0 M}$. This procedure was performed on the hysteresis loops of several $Fe_xCo_yMn_z$ films with different compositions. Details of the growth and composition determination are reported elsewhere.[4] The hysteresis loops were acquired using the VSM option of the Quantum Design Physical Properties Measurement System (PPMS) calibrated by the NIST Pd standard. The hysteresis had a linear, diamagnetic background removed (from the MgO substrate) and was smoothed with a Gaussian filter. The results of these fits are presented in Table I.

These values are on the same order as epitaxial bcc Fe(100) on GaAs(100),[20] epitaxial bcc Co on GaAs(110),[21] and epitaxial bcc Co on GaAs(001)[22] cubic anisotropies, which were found by ar-FMR to be $2.4 \cdot 10^4$ J/m^3, $-6.6 \cdot 10^4$ J/m^3, and $2.6 \cdot 10^4$ J/m^3, respectively. The anisotropy constants in these cases were found to depend on film thickness.

TABLE I. Cubic anisotropy constant K_1 from fitting Stoner–Wohlfarth model calculated hysteresis loops to VSM measured hysteresis loops for bcc $Fe_xCo_yMn_z$ films.

x	y	z	$M(10^{-7}$ A m$^2)$	$K_1(10^4$ J/m$^3)$
0.33	0.60	0.07	1.1 ± 0.1	2.7 ± 0.1
0.43	0.47	0.10	1.3 ± 0.1	2.3 ± 0.1
0.43	0.46	0.11	2.3 ± 0.1	6.3 ± 0.3
0.47	0.42	0.12	1.7 ± 0.1	3.9 ± 0.2
0.40	0.42	0.18	2.4 ± 0.1	4.1 ± 0.2

V. CONCLUSIONS

The Stoner–Wohlfarth model calculated hysteresis loops computationally coupled with a least-squares fitting algorithm and some simple data filtering techniques create a viable method for determining anisotropy constants from magnetic hysteresis data. Not only can cubic anisotropy constants be determined but a similar technique can also be applied to more complicated energies to predict their hysteresis behavior as well (including higher order anisotropy terms, surface/interface anisotropy contributions, fringe field interactions, etc.). For example, second-order, K_2, cubic anisotropy could be considered for hysteresis loops measured near the [111] crystal plane. This also opens the possibility of quantifying effects that contribute to a hysteresis other than these anisotropies including interlayer coupling between a free layer and a pinned layer magnetization[18] with a single fitting procedure.

This technique has been shown to extract cubic anisotropy constants, in good agreement with known first-order cubic anisotropies presented in the literature. However, it is not without its limitations; square hysteresis loops acquired along the easy axis cannot be used. Experience shows that hysteresis data taken at angles near the central angle between the easy and hard axes of the sample achieve the best results for the extraction of the fit parameters.

The sample must have reached its saturation magnetization from a sufficiently large applied magnetic field so that the macroscopic spin approximation is valid. Simultaneously fitting hysteresis loops taken at a few angles for the same sample could improve the anisotropy determination further. Despite requiring hysteresis measurements to be taken at several angles, this technique would require data to be taken at far fewer angles than ar-FMR techniques, which typically require data to be taken roughly every 5°.

In previous combinatorics studies,[7–9] the anisotropy constants of many alloys have only been characterized qualitatively in favor of easily studying measurement of magnetic properties such as the coercive field and the saturation magnetization. These are typically determined from the hysteresis of the sample measured either with a VSM or a MOKE magnetometer, the data of which can be retroactively used to determine magnetic anisotropy constants as well. However, determining the anisotropy constants of these materials may require modifications of the energy equation to include different orders of anisotropy, such as uniaxial anisotropy (both perpendicular shape anisotropy and in-plane uniaxial anisotropy generated from details of the film growth) or second-order cubic terms; fortunately, the analysis process would remain relatively unchanged. Coupled with a machine-learning algorithm,[12,13] these data and the relevant composition data of the samples could be used to predict new magnetic materials.

ACKNOWLEDGMENTS

This work was supported by the National Science Foundation through Grant No. 1809846. We would like to thank Collin Crites and Frank Schooner for useful discussions and suggesting corrections to this manuscript.

DATA AVAILABILITY

The data that support the findings of this study are available from the corresponding author upon reasonable request.

REFERENCES

[1] B. Tudu *et al.*, "Recent developments in perpendicular magnetic anisotropy thin films for data storage applications," Vacuum **146**, 329 (2017).
[2] W. Kang *et al.*, "Modeling and exploration of the voltage-controlled magnetic anisotropy effect for the next-generation low-power and high-speed MRAM applications," IEEE Trans. Nanotechnol. **16**, 387 (2017).
[3] T. Burkert *et al.*, "Giant magnetic anisotropy in tetragonal FeCo alloys," Phys. Rev. Lett. **93**, 027203 (2004).
[4] R. J. Snow *et al.*, "Large moments in bcc $Fe_xCo_yMn_z$ ternary alloy thin films," Appl. Phys. Lett. **112**, 072403 (2018).
[5] G. A. Prinz, "Magnetic anisotropy in epitaxial metal films," Ultramicroscopy **47**, 346 (1992).
[6] J. Rigue *et al.*, "A torque magnetometer for thin films applications," J. Magn. Magn. Mater. **324**, 1561 (2012).
[7] S. W. Fackler *et al.*, "Combinatorial study of Fe-Co-V hard magnetic thin films," Sci. Technol. Adv. Mater. **18**, 231 (2017).
[8] T. R. Gao *et al.*, "Combinatorial exploration of rare-earth-free permanent magnets: Magnetic and microstructural properties of Fe-Co-W thin films," Appl. Phys. Lett. **102**, 022419 (2013).
[9] V. Alexandrakis *et al.*, "Combinatorial development of Fe–Co–Nb thin film magnetic nanocomposites," ACS Comb. Sci. **17**, 698 (2015).
[10] S. Vilain *et al.*, "Surface roughness and composition effects on the magnetic properties of electrodeposited Ni-Co alloys," J. Magn. Magn. Mater. **157–158**, 274 (1996).
[11] Y. P. Zhao *et al.*, "Effect of surface roughness on magnetic domain wall thickness, domain size and coercivity," J. Appl. Phys. **89**, 1325 (2001).
[12] A. G. Kusne *et al.*, "On-the-fly machine-learning for high-throughput experiments: Search for rare-earth-free permanent magnets," Sci. Rep. **4**, 6367 (2014).
[13] Y. Iwasaki *et al.*, "Machine learning autonomous identification of magnetic alloys beyond the Slater-Pauling limit," Commun. Mater. **2**, 31 (2021).
[14] J. Geshev *et al.*, "Dependence of the magnetization and remanence of single-domain particles on the second cubic anisotropy constant," J. Appl. Phys. **90**, 6243 (2001).
[15] J. Garcia-Otero *et al.*, "Influence of the cubic anisotropy constants on the hysteresis loops of single-domain particles: A Monte Carlo study," J. Appl. Phys. **85**, 2287 (1999).
[16] C. Daboo *et al.*, "Anisotropy and orientational dependence of magnetization reversal process in epitaxial ferromagnetic thin films," Phys. Rev. B **51**, 15964 (1995).
[17] N. A. Usov and S. E. Peschany, "Theoretical hysteresis loops for single-domain particles with cubic anisotropy," J. Magn. Magn. Mater. **174**, 247 (1997).
[18] M. Labrune *et al.*, "Magnetization rotation in spin-valve multilayers," J. Magn. Magn. Mater. **171**, 1 (1997).
[19] W. Wernsdorfer *et al.*, "Magnetisation reversal by uniform rotation (Stoner–Wohlfarth model) in FCC cobalt nanoparticles," J. Magn. Magn. Mater. **242–245**, 132 (2002).
[20] J. J. Krebs *et al.*, "Properties of Fe single-crystal films grown on (100)GaAs by molecular-beam epitaxy," J. Appl. Phys. **61**, 2596 (1987).
[21] G. A. Prinz *et al.*, "FMR of cubic cobalt grown by molecular beam epitaxy on GaAs," J. Appl. Phys. **57**, 3672 (1985).
[22] S. J. Blundell *et al.*, "Structure induced magnetic anisotropy behavior in Co/GaAs(001) films," J. Appl. Phys. **73**, 5948 (1993).